Application of experimental design methodology to optimize acetaminophen removal from aqueous environment by magnetic chitosan@multi-walled carbon nanotube composite: Isotherm, kinetic, and regeneration studies

Ebrahim Nabatian [a, b], Maryam Dolatabadi [c], Saeid Ahmadzadeh [d, e*]

[a] Student Research Committee, Kerman University of Medical Sciences, Kerman, Iran.
[b] Department of Chemistry, Faculty of Sciences, Shahid Bahonar University of Kerman, Kerman, Iran.
[c] Environmental Science and Technology Research Center, Department of Environmental Health Engineering, School of Public Health, Shahid Sadoughi University of Medical Sciences, Yazd, Iran.
[d] Pharmaceutics Research Center, Institute of Neuropharmacology, Kerman University of Medical Sciences, Kerman, Iran.
[e] Pharmaceutical Sciences and Cosmetic Products Research Center, Kerman University of Medical Sciences, Kerman, Iran

ABSTRACT

Acetaminophen is a widely used drug worldwide and is frequently detected in water and wastewater as a high-priority trace pollutant. This study investigated the applicability of the adsorption processes using a composite of magnetic chitosan and multi-walled carbon nanotubes (MCS@MWCNTs) as an adsorbent in the treatment of acetaminophen. The model was well fitted to the actual data, and the correlation coefficients of R^2 were 0.9270 and 0.8885, respectively. The maximum ACT removal efficiency of 98.1% was achieved at ACT concentration of 45 mg L^{-1}, pH of 6.5, MCS@MWCNTs dosage of 400 mg L^{-1}, and the reaction time of 23 min. The result shows that BET specific surface area of 640 m^2 g^{-1}. The adsorption isotherms were well fitted with the Langmuir Model (R^2 =0.9961), depicting the formation of monolayer adsorbate onto the surface of MCS@MWCNTs. The maximum monolayer adsorption capacity of 256.4 mg g^{-1} was observed for MCS@MWCNTs. The pseudo-second-order kinetic model well depicted the kinetics of ACT adsorption on MCS@MWCNTs (R^2=0.9972). Desorption studies showed that the desorption process is favored at high pH under Alkaline conditions. The results demonstrate that the MCS@MWCNTs is an efficient, durable, and sustainable adsorbent in water purification treatment.

1. Introduction

Pharmaceutical pollutants (PPs) are a group of emerging anthropogenic hazard contaminants that contain different groups of human and veterinary medicinal compounds that are used widely all over the globe [1, 2]. Acetaminophen (ACT) is one of the most frequently used drugs worldwide. ACT is a type of analgesic and antipyretic drug commonly used as a fever reducer and pain reliever. Because of high consumption worldwide, it is one of the most frequently detected drugs in bodies of water and wastewater [3-5]. Overdoses of ACT produce the accumulation of toxic metabolites, which may cause severe and sometimes fatal hepatoxicity, and nephrotoxicity; generally, due to their bio-accumulation, they pose a potential long-term risk

for aquatic and terrestrial organisms. To improve the water quality and protect human health, the water contaminated with emerging contaminants, including pharmaceuticals, must be efficiently treated using an appropriate technique before being supplied for consumption [6, 7]. Various physical, chemical, and biological technologies can be employed to treat ATC from water and wastewater. Among the different treatments, adsorption technology is attractive due to its effectiveness, efficiency, and economy. The common adsorbents primarily include activated carbons, zeolites, clays, industrial by-products, agricultural wastes, biomass, and polymeric materials. AC is characterized by high porosity and an extensive surface area, enabling it to adsorb many kinds of pollutants efficiently. Despite its high adsorption capacity, the use of AC on a large scale is limited by process engineering difficulties such as the dispersion of the AC powder and the cost of its regeneration. However, these adsorbents described above suffer from low adsorption capacities and separation inconvenience. Therefore, efforts are still needed to investigate new promising adsorbents [8]. Chitosan (CS) has gained considerable attention as a non-conventional adsorbent in water decontamination research due to its favorable properties such as non-toxicity, eco-friendliness, high availability, biodegradability, good biocompatibility, low cost, and good adsorption properties. However, the high solubility of CS at lower pH (i.e., below 4) and poor mechanic properties are the limiting problems for taking advantage of the interaction ability of CS with Pollutant molecules. Thus, it might be not advisable to use untreated CS as an adsorbent in aqueous media [9-12]. One good strategy is to immobilize CS on solid matrixes that can stabilize CS in acid solutions and improve its mechanical strength to overcome these problems. Different kinds of solid organic or inorganic matrixes have been used to form composites with CS, such as glass plates, activated clay, silica, and polymer spheres.

Recently, carbon nanotubes (CNTs) have also been used as a matrix to prepare CS/CNTs composites.

CNTs, a fascinating new member of the carbon family, have attracted strong research interest since their discovery because of their unique morphologies and various potential applications, as well as their remarkable mechanical properties [13]. CNTs have been proven to possess excellent adsorption capacity in removing organic and inorganic pollutants because of their hollow and layered nanosized structures with a large specific surface area. Also, CNTs can provide improved mechanical strength and better structural integrity conditions. However, the difficulty in collecting these adsorbents from treated effluents can cause inconveniences in their practical application. As an efficient, fast, and economical method for separating magnetic materials, Magnetic separation technology has received considerable attention in recent years. Imparting magnetic properties to adsorbents can isolate them from the medium using an external magnetic field without the need for complicated centrifugation or filtration steps [11, 14].

The current work aimed to investigate the efficacy of magnetic CS and multi-walled carbon nanotubes (MCS@MWCNTs) as the adsorbent in ACT removal under various operating conditions. Effective parameters on ACT removal such as solution pH, reaction time, ACT concentration, and adsorbent dosage were optimized with response surface method (RSM) using central composite design (CCD). In addition, some extra experiments were performed to study adsorption kinetics and isotherms, and adsorbent reusability.

2. Experimental
2.1. Chemicals
Chitosan (Merck), Multi-walled carbon nanotubes (Sigma-Aldrich), Acetaminophen ($C_8H_9NO_2$, Merck), Ferric chloride ($FeCl_3.6H_2O$, Merck), Sodium acetate ($C_2H_3NaO_2$ Merck), Ethylene glycol ($C_2H_6O_2$, Merck), Acetone (C_3H_6O, Merck), Paraffin (CnH_{2n+2}, Merck), Sodium hydroxide (NaOH, Merck), Hydrochloric acid (HCl, Merck), were of analytical grade. All solutions used in the experiments were prepared with distilled water.

2.2. Preparation of Fe₃O₄ nanoparticles

Typically, 1.35 g of $FeCl_3.6H_2O$ and 3.6 g of sodium acetate were dissolved in 40 mL ethylene glycol with stirring and heating simultaneously. The temperature has risen to 80-100 °C. After stirring for 30 min, the yellow-brown color solution was transferred to a Teflon-lined stainless-steel autoclave and heated in the oven at 180°C for 12 h. Then, the autoclave was allowed to cool down to room temperature naturally. The black magnetite particles were washed with acetone and water several times and dried in the oven at 60°C overnight [15].

2.3. Preparation of MCS@MWCNTs

The composites of MCS@MWCNTs were synthesized by a suspension cross-linking approach with some modification. Typically, 0.1 g of chitosan was dissolved in 20 mL of 2% (v/v) acetic acid solution under ultrasonication. Subsequently, 0.2 g of Fe_3O_4 and 0.2 g of MWCNTs were added into the chitosan solution, and the reaction system was further ultrasonicated for 20 min. Then, the above mixture was slowly dispersed in 40 mL of paraffin containing 2 mL of span-80 under stirring. After 30 min of emulsification, 1 mL of 25% (v/v) glutaraldehyde was introduced into the system for the cross-linking of chitosan. Then the mixture was stirred continuously for 1 h at 70 °C. Afterward, the pH value of the reaction solution was adjusted to 9–10 with 1 mol L^{-1} NaOH and the reaction system was allowed to stir for another 1 h at 80 °C. The particles were washed with petroleum ether, ethanol, and ultrapure water three times, respectively. Finally, MCS@MWCNTs were obtained by magnetic separation and freeze-dried for 12 h [16].

2.4. Characterization of MCS@MWCNTs

The standard BET equation was employed to calculate the Brunauer-Emmert-Teller (BET) surface area from the desorption isotherms. The pore size distribution was determined from desorption isotherms using the Barrett, Joyner, and Halenda (BJH) method. All calculations were performed automatically by an Accelerated Surface Area and Porosimeter system (ASAP 2010, Micromeritics, U.S.A.). The pH of zero point charge (pHzpc) describes the condition when the charge density on the surface is zero. It is usually determined concerning the pH of the mixtures. Researchers proposed a mass titration method to determine the values of pH_{zpc}: portions of 20 mL NaCl (0.01 M) solution were added into different flasks. The initial pH was adjusted with NaOH or HCl to the desired values between 2 and 12 (metrohm 827 pH/mV lab pH meter). Then, 20 mg of the MCS@MWCNTs sample was suspended into each flask. The flasks with caps were placed in a shaker. After shaking for 24 h, the pH of the solutions was measured and designated as pHfinal. The pH_{zpc} value is the point where the $pH_{initial}$ = pH_{final} [17].

2.5. Experimental design and statistical analysis

The response surface methodology (RSM) is a set of statistical and mathematical methods used to analyze experimental results. RSM is used in conditions that many input variables affect the performance and response characteristics of the process. A complete description of a process requires that it be modeled as a polynomial function generally of degree 2 or higher. Since operational conditions may be associated with changes, the nonlinear second-order model can describe it. The quadratic regression model was considered in the form of Equation 1[18-20]:

$$Y = \beta_0 + \sum_{i=1}^{k} \beta_1 X_1 + \sum_{i=1}^{K} \beta_{ii} X_i^2 + \sum_{i=1}^{K} \sum_{j=1}^{K} \beta_{jj} X_i X_j + \epsilon$$

(Eq. 1)

where Y represents the response of process, i and j index numbers for factors, X_i and X_j are the design variables, β_i and β_j represents the coefficient of first-order effect, β_{ij} is the coefficient of interaction, β_0 is constant-coefficient, k is the number of factors and ε is the model error. In this study, CCD is based on a four-factor design, including ACT concentration (X_1), pH (X_2), adsorbent dosage (X_3), and reaction time (X_4) were discussed. In the

Table 1. Coded and actual values of independent process variables used in the design
of an experimental matrix using the RSM-CCD framework.

Coded Variables (X_i)	Factors	Coded Level				
		$-\alpha$	-1	0	$+1$	$+\alpha$
X_1	A= ACT Concentration (mg L^{-1})	20.0	40.0	60.0	80.0	100.0
X_2	B= pH	4.00	5.50	7.00	8.50	10.00
X_3	C= Adsorbent dosage (mg L^{-1})	100	200	300	400	500
X_4	D= Reaction time (min)	5.00	11.25	17.50	23.75	30.00

design of the experiments, each variable with five levels was considered, in accordance with Table 1. The statistical significance of CCD modeling parameters and their combined interactions at certain levels were examined based on their p values. Analysis of variance (ANOVA) was used to check the experimental data and accuracy of the response surface model. The coefficient of variation (C.V. %) and R^2 values was calculated to evaluate the goodness of fit of the regression model. The model precision associated with the range of predicted values at the given points was also elucidated.

2.6. Adsorption experiments

All adsorption experiments were carried out in 100 mL of pyrex reactor by mixing a given dose of MCS@MWCNTs with a certain concentration of ATC solution in a thermostatic shaker. The initial pH of the ACT solution was adjusted to a certain value using NaOH and HCl solution by pH meter. After adsorption, the mixture was immediately centrifuged, and the supernatant was analyzed for the concentration of ATC was measured using a UV/Vis spectrophotometer (Optizen). The wavelength corresponding to the maximum absorbance of ATC was 242 nm. Each experiment was repeated at least three times, and the average value was recorded. The ACT removal (q_e) and adsorption capacity were calculated by Equations (2) and (3), respectively [15, 21]:

$$\text{ACT Removal (\%)} = \frac{C_0 - C_t}{C_0} \times 100 \quad (Eq. 2)$$

$$q_e = \frac{(C_0 - C_e) \times V}{m} \quad (Eq. 3)$$

Where C_0 is the initial ACT concentration (mg L^{-1}), C_e is the ACT concentration (mg L^{-1}) after the batch adsorption procedure, m is the adsorbent dosage (g L^{-1}), and q_e is the amount of ACT adsorbed by the adsorbent (mg g^{-1}).

2.7. Kinetic and isotherm models

Two widely used kinetics models, pseudo-first-order and pseudo-second-order models were examined to fit the experimental data. The linear expression of pseudo-first-order and pseudo-second-order models are expressed as Equation 4 and 5 [15, 22].

$$\ln(q_e - q_t) = \ln(q_e) - k_1 t \quad (Eq. 4)$$

$$\frac{t}{q_t} = \frac{1}{k_2 q_e^2} + \frac{t}{q_e} \quad (Eq. 5)$$

where k_1 (min^{-1}) is the rate constant of the pseudo-first-order, k_2 (g mg^{-1} min^{-1}) is the second-order rate constant. q_e and q_t (mg g^{-1}) are the adsorption capacities at equilibrium and time t (min), respectively.

Three commonly used isotherm models, the Langmuir and Freundlich isotherms, are selected to analyze the equilibrium experimental data for the adsorption of ACT onto MCS@MWCNTs. The two models are given as Equation 6 and 7 [23].

$$\frac{C_e}{q_e} = \frac{C_e}{q_m} + \frac{1}{bq_m} \quad (Eq. 6)$$

$$\ln q_e = \ln K_F + \left(\frac{1}{n}\right) \ln C_e \quad (Eq. 7)$$

where C_e (mg L^{-1}) is the equilibrium concentration of the ACT, q_e (mg g^{-1}) is the amount of ACT
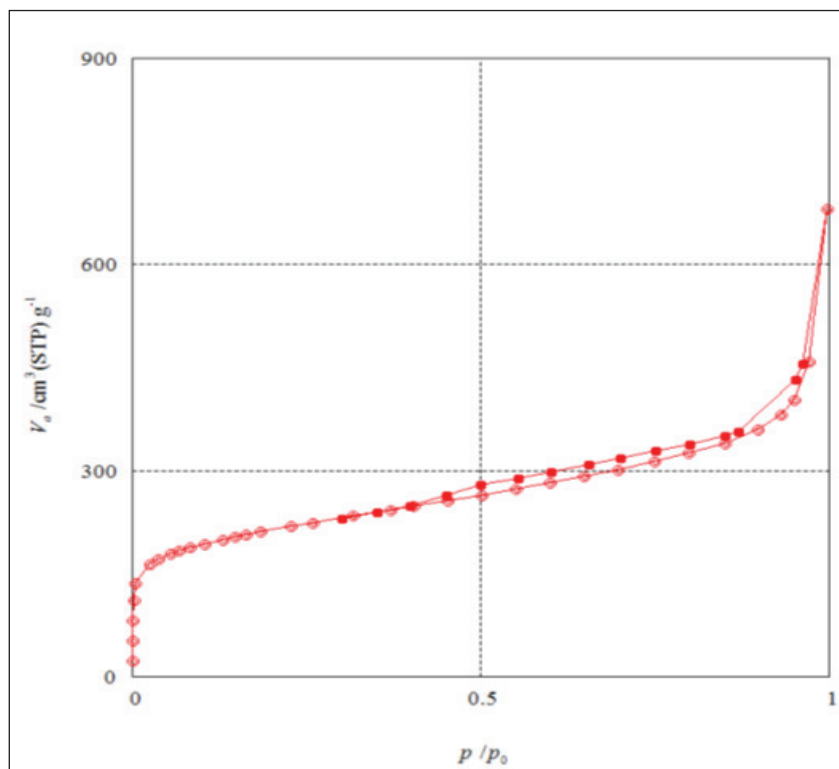
Fig. 1. N$_2$ adsorption–desorption isotherms of MCS@MWCNTs.

adsorbed under equilibrium, b (L mg^{-1}) is the Langmuir adsorption constant, and q$_m$ (mg g^{-1}) is the maximum adsorption amount. K$_F$ and n are Freundlich constants. n presents the adsorption intensity, assessing the unfavorable adsorption (n<1) or preferential adsorption (n > 1), and K$_F$ ((mg g^{-1} (L mg^{-1})$^{1/n}$) is the adsorption capacity of the adsorbent.

The isotherm can predict if an adsorption system is favorable or unfavorable. Researchers pointed out that the essential characteristics of the Langmuir isotherm can be expressed in terms of a dimensionless constant, R$_L$, as presented in Equation 8.

$$R_L = \frac{1}{1+bC_0} \qquad (Eq.\ 8)$$

where, R$_L$ is the separation factor or equilibrium parameter, which is a direct function of the Langmuir constant b. The values of R$_L$ indicate the shape of the isotherm: R$_L$>1 (unfavorable), R$_L$ =1 (linear), 1 > R$_L$ > 0 (favorable) and R$_L$ = 0 (irreversible).

3. Results and discussions
3.1. Characterization of adsorbent
Figure 1 shows the N$_2$ adsorption-desorption isotherms of MCS@MWCNTs. According to Figure 1, the N$_2$ adsorption nearly completed at a lower relative pressure of P/P$_0$ < 0.1, suggesting that the sample has the micropore size distribution. In addition, the N$_2$ hysteresis loop at P/P$_0$ > 0.5 was observed, indicating the presence of mesopores structure. Accordingly, the micropore volume fraction is higher than 79%, confirming the majority of micropores. The MCS@MWCNTs had a high BET-specific surface area of 640 m^2 g^{-1}.

The adsorbent's pH$_{zpc}$ value was determined to explain the adsorption behavior. This parameter reveals the characteristics of the surface's active sites in a linear range of solution pH. The pH$_{zpc}$ of MCS@MWCNTs was found to be around 6.8, implying that the surface of the adsorbent would be positively charged at solution pH below 6.8 and negatively charged at solution pH above 6.8. Hence, one can conclude that adsorption of cationic molecules is favored at pH>6.8, while anionic molecules adsorption is favored at pH < 6.8.

3.2. Development and analysis of regression model equation

CCD is considered a reliable method to analyze diagnostic plots, such as the normal probability plot of residuals and to predict versus actual values, to validate the adequacy of the model. The normal probability plot of the studentized residuals is an excellent graphical representation for the diagnosis of data normality (Fig. 2). The data were well fitted with the line. In addition, the residuals followed a random distribution around zero with a variation of ±3.0 (Fig. 3).
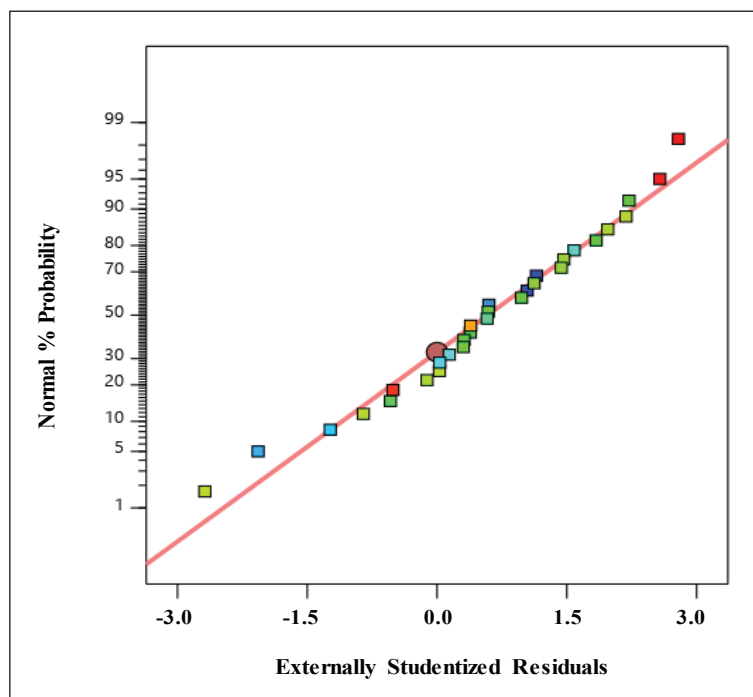
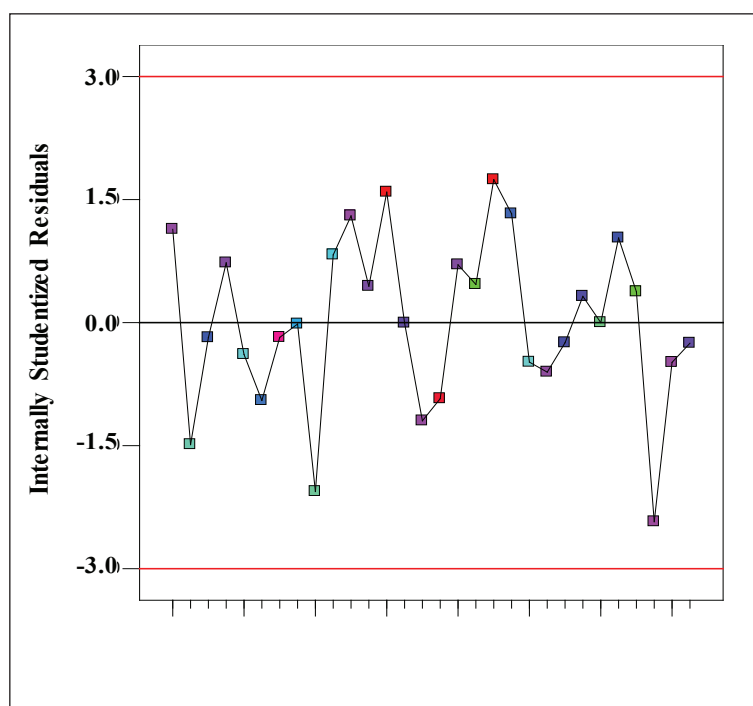**Fig. 2.** Normal probability plot of the internally studentized residuals for ACT removal.

Fig. 3. Run number versus residual data for ACT removal.

The result indicates that the data were normally distributed in the model response. In addition, the corresponding relationship between the residual and the predicted value of the equation also could reflect the reliability of the model. When the points are distributed discretely in the Figure, it could represent the higher reliability of the model.

ANOVA carried out the analysis of obtained experimental data. Table 2 shows ANOVA data for the removal efficiency (Y). F-value in ANOVA implies that the model is significant for the dependent variable. As shown in Table 2, F-value is 87.47 for removal efficiency, which indicates the model is significant. Prob>F or p-value less than 0.05 demonstrates that these model terms are important. The lack of fit F-value of 4.13 with the associated p-value of 0.0612 for the response was insignificant due to relative pure error. The validity of the model is checked by some statistical parameters, including the determination coefficient (R^2), adjusted R^2, predicted R^2, adequate precision (AP), and coefficient of variation (CV). R^2 is defined as a measure of the degree of fit. As R^2 approaches unity, the degree of fit increases.

The similarity between R^2 and adjusted R^2 shows the model's compatibility to predict the dependent variable. The difference between predicted R^2 and

adjusted R^2 must be less than 0.2. It is indicated that predicted R^2 is in acceptable agreement with adjusted R^2. AP is defined as a measure of the ratio of the signal to noise. A ratio greater than 4 is desirable. In our current study, all findings in Table 2 were acceptable, which confirmed the model's fitness with the experimental results.

Overall, the ANOVA analysis was reliable to optimize and determine the level of each factor for removal ACT. Therefore, it is pretty satisfactory to predict the ACT removal efficiency by the second-order polynomial model. In the present study, five model terms (X_1(ACT concentration), X_2(pH), X_3(Adsorbent dosage), X_4(Reaction time), X_2^2(quadratic effect of pH)) was most important because of their p-values less than 0.05. These model terms are shown in the model equation. Based on ANOVA results, the empirical model equation in terms of coded variables was developed for the removal efficiency as Equation 9.

$$Y(\%) = 82.72 - 4.84X_1 - 3.27X_2 + 5.71X_3 + 5.57X_4 - 3.87X_2^2$$

(Eq. 9)

The positive sign in the equation indicates the synergistic effect of the corresponding factor on the response, and the negative sign represents

Table 2. Analysis of variance (ANOVA) for regression model.

Source	Sum of Squares	Degree of freedom (df)	Mean Squares	F-Value	Probability P-value > F
Model	2775.21	5	555.04	87.47	< 0.0001
	561.89	1	561.89	88.55	< 0.0001
	256.30	1	256.30	40.39	< 0.0001
	781.29	1	781.29	123.12	< 0.0001
	744.41	1	744.41	117.31	< 0.0001
	431.33	1	431.33	67.97	< 0.0001
Residual	152.30	24	6.35	-	-
Lack of Fit	143.18	19	7.54	4.13	0.0612
Pure Error	9.12	5	1.82	-	-
Cor Total	2927.51	29	-	-	-
Fit Statistics					
R^2	0.9480		SD	2.52	
Adjusted R^2	0.9371		CV	3.16	
Predicted R^2	0.9140		AP	34.40	

the antagonistic effect. The effect of the initial concentration (20-100 mg L^{-1}) was investigated. The removal efficiency for ACT is highly dependent on the initial ACT concentration. Figure. 4 illustrated that removal efficiency decreases from 92.3 to 72.6%, increasing ACT concentration from 20 to 100 mg L^{-1}. The effect of initial ACT concentration depends on the immediate relation between the concentration of the ACT and the available sites on an adsorbent surface. In general, the removal efficiency decreases with an increase in the initial ACT concentration due to the saturation of adsorption sites on the adsorbent surface. On the other hand, the increase in initial ACT concentration will cause an increase in the capacity of the adsorbent, which may be due to the high driving force for mass transfer at a high initial ACT concentration.

Figure 4 shows the effect of solution pH ranging from 4 to 10 on the adsorption of ACT onto MCS@ MWCNTs. Figure 4 implies that the adsorption of

ACT onto MCS@MWCNTs at pH solution between 4 and 7.0 is a pH-dependent phenomenon, so the adsorption performance was around 85% in all pH ranges. The increase of solution pH to 7.0 caused improvement of the adsorption. A decreasing trend in adsorption of ACT was observed for the solution pH over 7.0. Accordingly, the optimum solution pH at which the maximum adsorption of the ACT under the selected experimental conditions was obtained was found to be 6.5. The effect of solution pH on the adsorption of ACT onto MCS@ MWCNTs can be justified considering the pHzpc of MCS@MWCNTs (6.8) and pK$_a$ of ACT (9.4). According to Figure 4, the adsorption of ACT onto MCS@MWCNTs is almost independent of solution pH over the solution pHs between 4.0 and 7.0. At this pH range, the ACT molecules remain mostly neutral and nonionic and thus unfavorable for electrostatic and π-π interactions with the functional groups on the surface of MCS@MWCNTs. Therefore, the hydrophobic
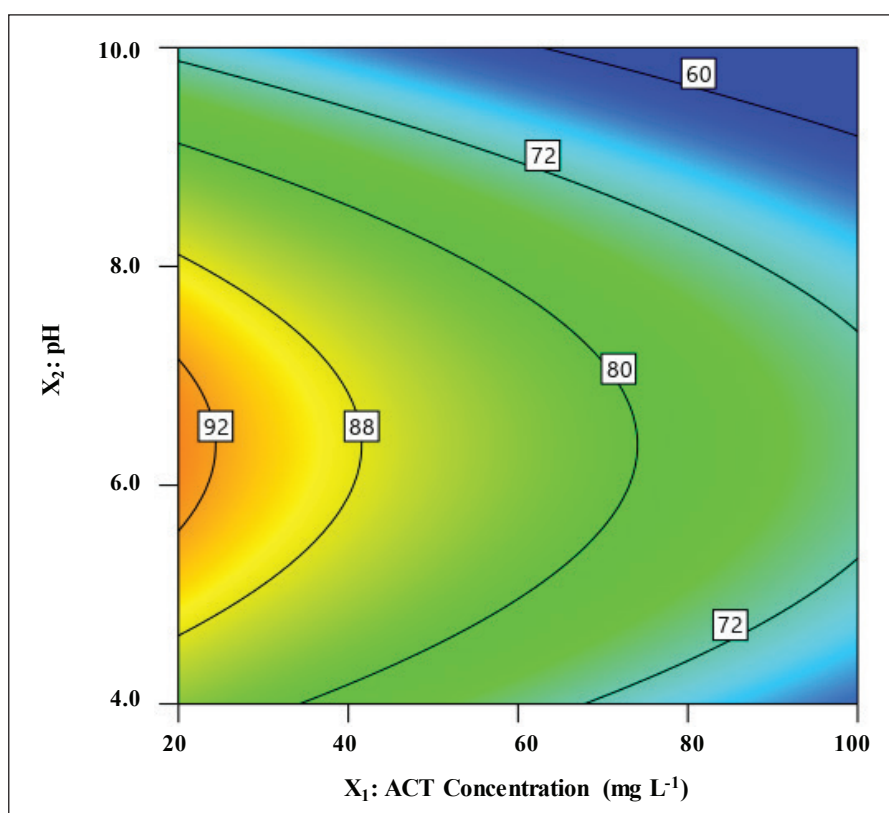

Fig. 4. Contour plot of ACT removal showing the effect of variables of ACT concentration and pH (MCS@MWCNTs dosage of 300 mg L^{-1} and reaction time of 17.5 min).
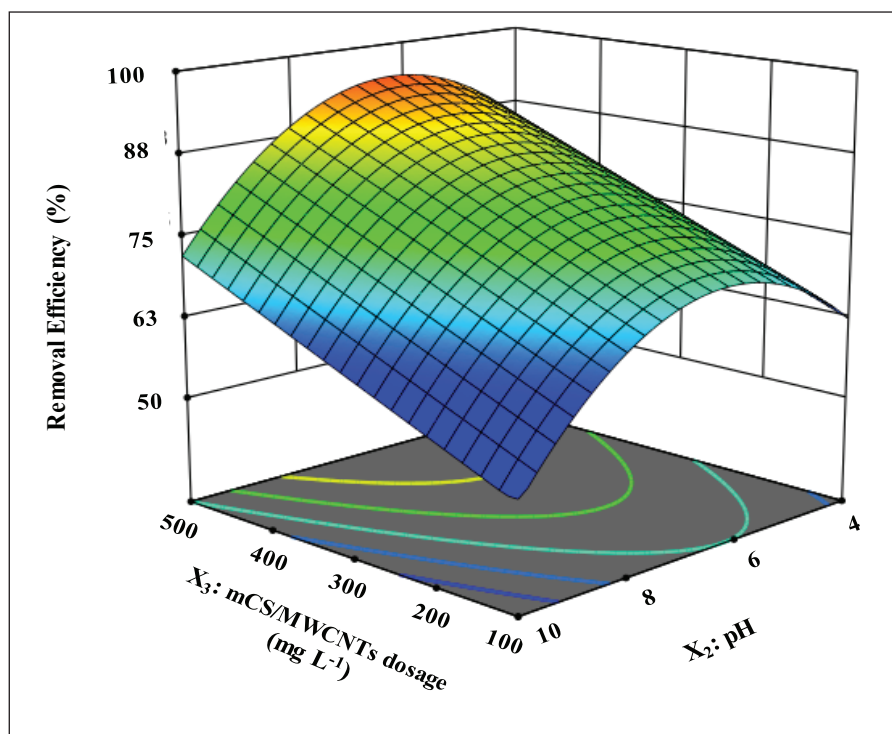
Fig. 5. Response surface plot of ACT removal showing the effect of variables of MCS@MWCNTs dosage and pH (ACT concentration of 60 mg L^{-1} and reaction time of 17.5 min).

interactions might be the primary mechanism anticipated in the ACT adsorption under these conditions. Considering that the pK$_a$ of ACT is 9.4, the main fraction of ACT molecules was in anionic form at solution pHs above this value. In contrast, the surface of MCS@MWCNTs (pH$_{zpc}$ = 6.8) is negatively charged at alkaline solution pH. Therefore, the reduction of ACT adsorption at the pH over 7.0 can be related to the electrostatic repulsion that occurred between anionic ACT molecules and the negatively charged functional groups on the surface of MCS@MWCNTs. This effect tends to enhance the adsorption of ACT onto MCS@MWCNTs. The greater the solution pH over 7.0, the more negative the surface of MCS@MWCNTs and the more ionized the ACT molecules. Therefore, the greater the repulsive force leads to reduced adsorption. The MCS@MWCNTs dosage as adsorbent was one of the dominant parameters controlling the adsorption of ACT. The relation of MCS@MWCNTs dosage and pH on removal efficiency of ACT is illustrated in Figure 5. Increasing MCS@MWCNTs dosage from 100 to 500 mg L^{-1} leads to an improvement in ACT removal efficiency from 71.4% to 94.2% at ACT concentration of 60 mg L^{-1}, pH of 7, and reaction time 17.5 min. The increase in removal efficiency with increasing adsorbent dose is probably due to the greater adsorbent surface area and pore volume available at higher adsorbent dose providing more functional groups and active adsorption sites that result in higher removal efficiency.

The dependence of the removal efficiency of ACT on reaction time is shown in Figure 6. This Figure shows that removal efficiency increases with time, and adsorption reaches equilibrium in about 25 minutes. It indicates that the rapid increase in removal efficiency is achieved during the first 20 min. The fast adsorption at the initial stage may be due to the higher driving force making an immediate transfer of adsorbate ions to the surface of MCS@MWCNTs particles and the availability of the uncovered surface area and the remaining active sites on the adsorbent. According to the results, an equilibrium time was set to 25 min for adsorption of ACT onto MCS@MWCNTs.
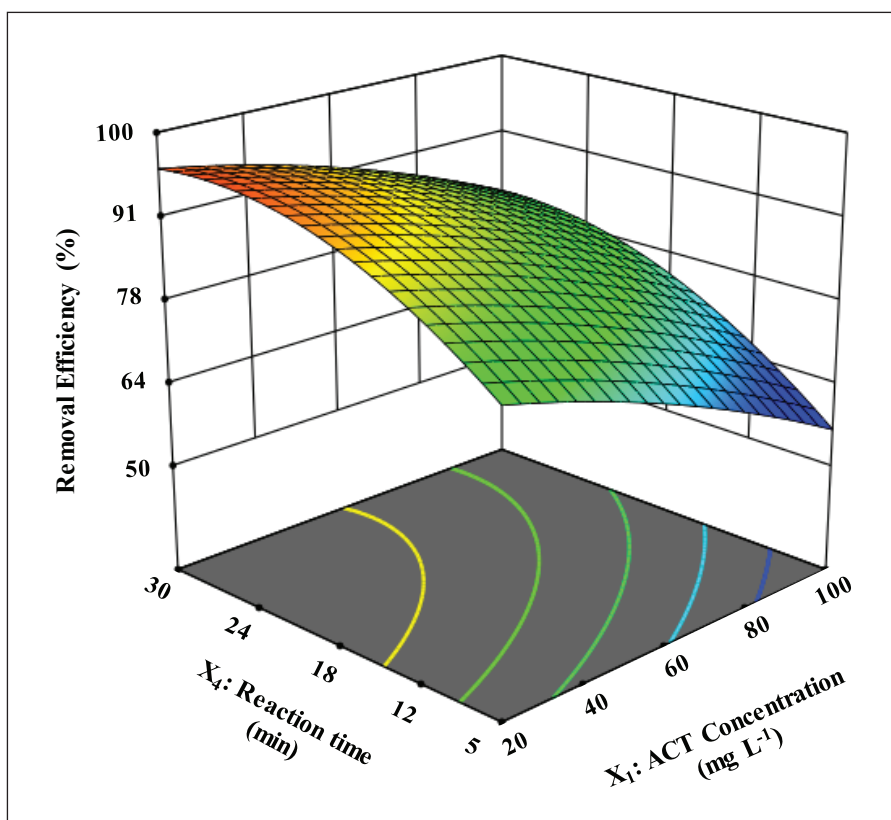
Fig. 6. Response surface plot of ACT removal showing the variables effect of reaction time and ACT concentration (MCS@MWCNTs dosage of 300 mg L^{-1}, and pH of 7).

3.3. Optimization and validation test

The optimization of operating conditions was conducted to determine the optimum values of these parameters required to achieve the highest ACT removal efficiency. Optimization was performed by numerical technique built in the Design-Expert software. The desired goal for the variables was chosen as "in range", while removal efficiency (response) was chosen as "maximize". According to the output results, the removal efficiency of ACT could reach a maximum value of 98.1% with the ACT concentration of 45 mg L^{-1}, pH of 6.5, MCS@MWCNTs dosage of 400 mg L^{-1}, and the reaction time of 23 min. An additional experiment was conducted to validate the model prediction (the optimal conditions) in this study. It was found that the results were greatly agreed with the predicted value through the quadratic model (Table 3). The experimental data were close to predicted data, indicating the accurate prediction ability of the model.

3.4. Adsorption kinetics and isotherms studies

The calculated kinetic parameters for pseudo-first-order and pseudo-second-order models are listed in Table 4. The pseudo-second-order model's correlative coefficient (R^2) was better than that of the pseudo-first-order model. These results indicated that the kinetic data fitted well with pseudo-second-order models. The pseudo-second-order model assumes that the rate-limiting step might be chemical adsorption in the adsorption process.

The adsorption isotherm is critically important in designing an adsorption system. The sorption data were fitted by the Langmuir and Freundlich equations, and the calculated parameters are

Table 3. Optimization and validation tests for ACT removal efficiency.

NO	ACT concentration (mg L^{-1})	pH	MCS@MWCNTs dosage (mg L-1)	Reaction time (min)	Experimental removal efficiency (%)	Predicted removal efficiency (%)
I	45	6.5	400	23	98.7	98.1
II	60	7.0	300	18	84.5	85.3
III	40	8.5	400	12	79.4	80.0
IV	80	8.5	200	25	71.0	69.4

Table 4. Parameters of kinetic equations for the adsorption of ACT.

Pseudo-First-Order model			Pseudo-Second-Order model		
q_e(mg g^{-1})	k_1(min^{-1})	R^2	q_e(mg g^{-1})	k_2 (g mg^{-1} min^{-1})	R^2
121.47	0.0689	0.9452	217.4	0.0008	0.9972

Table 5. Langmuir and Freundlich constants for the adsorption of ACT.

Langmuir				Freundlich		
q_m (mg g^{-1})	b (L mg^{-1})	R_L	R^2	K_f (L g^{-1})	n	R^2
256.4	0.658	0.026	0.9961	103.1	3.52	0.9542

summarized in Table 5. It was found that the Langmuir model provided a better fit to the observed data for the ACT, with high correlation coefficients (R^2=0.996). The maximum ACT sorption capacity (q_m) was 256.4 mg g^{-1}. The values of n and R_L were obtained at 3.52 and 0.026, respectively, suggesting that the adsorbent was favorable for removing ACT from the aqueous solution.

3.5. Regeneration studies

Desorption studies are necessary to complete the investigation of the mechanism involved in the adsorption of an adsorbate by an adsorbent and to regenerate the adsorbent for economic success. In the present study, desorption was explored, varying the pH from 4.0 to 10.0 and keeping the adsorbent dosage constant at 300 mg L^{-1}. An increase in pH favored ACT desorption from MCS@MWCNTs because of electrostatic repulsion between negatively charged sites on the adsorbent surface and ACT molecules. The feasibility of using MCS@MWCNTs in successive adsorption-desorption cycles was examined by contacting 45 mg L^{-1} ACT solution with 400 mg L^{-1} recycled adsorbent at pH 10.0. Under these conditions, ACT removal by MCS@MWCNTs and recycled MCS@MWCNTs was 98.1% and 86.7%, respectively. Such a marked loss of sorption capacity suggests that the reuse of desorbed MCS@MWCNTs would need some regeneration before recycling.

4. Conclusions

The process was optimized using central composite design (CCD), a statistical tool used to optimize response surface methodology (RSM). A second-order polynomial model adequately fit the experimental data with an adjusted R^2 of 0.9270, showing that the model could efficiently predict the ACT removal. It was found that all selected variables significantly affect ACT removal efficiency. Under these conditions, the maximum adsorption capacity for MCS@MWCNTs was found to be 256.4 mg g^{-1}. The results showed that the Langmuir and the pseudo-second-order kinetic models presented better fittings for the adsorption equilibrium and kinetics data. This study showed that MCS@MWCNTs are a useful adsorbent for the removal of ACT from aqueous solutions.

6. References

[1] B. Zaied, M. Rashid, M. Nasrullah, A. Zularisam, D. Pant, L. Singh, A comprehensive review on contaminants removal from pharmaceutical wastewater by electrocoagulation process, Sc. Total Environ., 726 (2020) 138095. https://doi.org/10.1016/j.scitotenv.2020.138095.

[2] A. Kumar, M. Chandel, A. Sharma, M. Thakur, A. Kumar, D. Pathania, L. Singh, Robust visible light active PANI/LaFeO3/CoFe2O4 ternary heterojunction for the photo-degradation and mineralization of pharmaceutical effluent: Clozapine, J. Environ. Chem. Eng., 9 (2021) 106159. https://doi.org/10.1016/j.jece.2021.106159.

[3] C.-C. Su, C.A. Cada Jr, M.L.P. Dalida, M.-C. Lu, Effect of UV light on acetaminophen degradation in the electro-Fenton process, Sep. Purif. Technol., 120 (2013) 43-51. https://doi.org/10.1016/j.seppur.2013.09.034.

[4] E. Bailey, H. Worthington, P. Coulthard, Ibuprofen and/or paracetamol (acetaminophen) for pain relief after surgical removal of lower wisdom teeth, a Cochrane systematic review, British Dent. j., 216 (2014) 451. https://doi.org/10.1038/sj.bdj.2014.330.

[5] M. Qutob, M. Rafatullah, M. Qamar, H.S. Alorfi, A.N. Al-Romaizan, M.A. Hussein, A review on heterogeneous oxidation of acetaminophen based on micro and nanoparticles catalyzed by different activators, Nanotechnol. Rev., 11 (2022) 497-525. https://doi.org/10.1515/ntrev-2022-0030.

[6] S. Wang, J. Wu, X. Lu, W. Xu, Q. Gong, J. Ding, B. Dan, P. Xie, Removal of acetaminophen in the Fe2+/persulfate system: Kinetic model and degradation pathways, Chem. Eng. J., 358 (2019) 1091-1100. https://doi.org/10.1016/j.cej.2018.09.145.

[7] H.N.P. Vo, G.K. Le, T.M.H. Nguyen, X.-T. Bui, K.H. Nguyen, E.R. Rene, T.D.H. Vo, N.-D.T. Cao, R. Mohan, Acetaminophen micropollutant: Historical and current occurrences, toxicity, removal strategies and transformation pathways in different environments, Chemosphere, 236 (2019) 124391. https://doi.org/10.1016/j.chemosphere.2019.124391.

[8] Z.B. Khalid, M. Nasrullah, A. Nayeem, Z.A. Wahid, L. Singh, S. Krishnan, Application of 2D graphene-based nanomaterials for pollutant removal from advanced water and wastewater treatment processes, in: Adapting 2D Nanomaterials for Advanced Applications, ACS Publications, ACS Symposium Series, 1353 (2020) 191-217.

https://doi.org/10.1021/bk-2020-1353.ch009.

[9]   I. Mustafa, Methylene blue removal from water using H2SO4 crosslinked magnetic chitosan nanocomposite beads, Microchem. J., 144 (2019) 397-402. https://doi.org/10.1016/j.microc.2018.09.032.

[10] H. Zeng, L. Wang, D. Zhang, P. Yan, J. Nie, V.K. Sharma, C. Wang, Highly efficient and selective removal of mercury ions using hyperbranched polyethylenimine functionalized carboxymethyl chitosan composite adsorbent, Chem. Eng. J., 358 (2019) 253-263. https://doi.org/10.1016/j.cej.2018.10.001.

[11] S. Wang, Y.-Y. Zhai, Q. Gao, W.-J. Luo, H. Xia, C.-G. Zhou, Highly efficient removal of acid red 18 from aqueous solution by magnetically retrievable chitosan/carbon nanotube: batch study, isotherms, kinetics, and thermodynamics, J. Chem. Eng. Data, 59 (2014) 39-51. https://doi.org/10.1021/JE400700C.

[12] M. Abbas, M. Arshad, M. Rafique, A. Altalhi, D. Saleh, M. Ayub, S. Sharif, M. Riaz, S. Alshawwa, N. Masood, Chitosan-polyvinyl alcohol membranes with improved antibacterial properties contained Calotropis procera extract as a robust wound healing agent, Arab. J. Chem., (2022) 103766. https://doi.org/10.1016/j.arabjc.2022.103766.

[13] M. Jawaid, A. Ahmad, N. Ismail, M. Rafatullah, Environmental remediation through carbon based nano composites, Springer, 2021. https://www.springer.com/series/8059

[14] K. Li, Q. Gao, G. Yadavalli, X. Shen, H. Lei, B. Han, K. Xia, C. Zhou, Selective adsorption of Gd3+ on a magnetically retrievable imprinted chitosan/carbon nanotube composite with high capacity, ACS Appl. Mater. Interfaces, 7 (2015) 21047-21055. https://doi.org/10.1021/acsami.5b07560.

[15] F. Jamali-Behnam, A.A. Najafpoor, M. Davoudi, T. Rohani-Bastami, H. Alidadi, H. Esmaily, M. Dolatabadi, Adsorptive removal of arsenic from aqueous solutions using magnetite nanoparticles and silica-coated magnetite nanoparticles, Environ. Prog. Sustain. Energy, 37 (2018) 951-960. https://doi.org/10.1002/ep.12751.

[16] K. Xu, Y. Wang, H. Zhang, Q. Yang, X. Wei, P. Xu, Y. Zhou, Solid-phase extraction of DNA by using a composite prepared from multiwalled carbon nanotubes, chitosan, Fe$_3$O$_4$ and a poly (ethylene glycol)-based deep eutectic solvent, Microchim. Acta, 184 (2017) 4133-4140. https://doi.org/10.1007/s00604-017-2444-4.

[17] H. Alidadi, M. Dolatabadi, M. Davoudi, F. Barjasteh-Askari, F. Jamali-Behnam, A. Hosseinzadeh, Enhanced removal of tetracycline using modified sawdust: optimization, isotherm, kinetics, and regeneration studies, Process Saf. Environ. Prot., 117 (2018) 51-60. https://doi.org/10.1016/j.psep.2018.04.007.

[18] A. Fegousse, A. El Gaidoumi, Y. Miyah, R. El Mountassir, A. Lahrichi, Pineapple bark performance in dyes adsorption: optimization by the central composite design, J. Chem., 2019 (2019) 3017163. https://doi.org/10.1155/2019/3017163.

[19] R.A. Khera, M. Iqbal, A. Ahmad, S.M. Hassan, A. Nazir, A. Kausar, H.S. Kusuma, J. Niasr, N. Masood, U. Younas, Kinetics and equilibrium studies of copper, zinc, and nickel ions adsorptive removal on to Archontophoenix alexandrae: conditions optimization by RSM, Desalin. Water Treat., 201 (2020) 289-300. https://doi.org/10.5004/dwt.2020.25937.

[20] V.U. Siddiqui, A. Ansari, M.T. Ansari, M. Akram, W.A. Siddiqi, A.M. Alosaimi, M.A. Hussein, M. Rafatullah, Optimization of facile synthesized ZnO/CuO nanophotocatalyst for organic dye degradation by visible light irradiation using response surface methodology, Catalysts, 11 (2021) 1509. https://doi.org/10.3390/catal11121509.

[21] S. Noreen, S. Ismail, S.M. Ibrahim, H.S.

Kusuma, A. Nazir, M. Yaseen, M.I. Khan, M. Iqbal, ZnO, CuO and Fe_2O_3 green synthesis for the adsorptive removal of direct golden yellow dye adsorption: kinetics, equilibrium and thermodynamics studies, Z. fur Phys. Chem., 235 (2021) 1055-1075. https://doi.org/10.1515/zpch-2019-1599.

[22] A. Kausar, K. Naeem, M. Iqbal, H.N. Bhatti, A. Ashraf, A. Nazir, H.S. Kusuma, M.I. Khan, Kinetics, equilibrium and thermodynamics of dyes adsorption onto modified chitosan: a review, Z. fur Phys. Chem., (2021). https://doi.org/10.1515/zpc-2019-1586.

[23] P. Mishra, Z.A. Wahid, R.M. Zaid, S. Rana, S. Tabassum, A. Karim, L. Singh, M.A. Islam, X. Jaing, M. Sakinah, Kinetics and statistical optimization study of bio-hydrogen production using the immobilized photobacterium, Biomass Convers. Biorefin., (2020) 1-12. https://doi.org/10.1007/s13399-020-00835-6.